J. Chem. Sci. (2018) 130:105
https://doi.org/10.1007/s12039-018-1509-1

REGULAR ARTICLE

Mechanisms of scavenging superoxide, hydroxyl, nitrogen dioxide and methoxy radicals by allicin: catalytic role of superoxide dismutase in scavenging superoxide radical

MANISH KUMAR TIWARI[a], NIHAR RANJAN JENA[b] and PHOOL CHAND MISHRA[a,*]

[a]Department of Physics, Institute of Science, Banaras Hindu University, Varanasi 221 005, Uttar Pradesh, India
[b]Discipline of Natural Sciences, Indian Institute of Information Technology, Design and Manufacturing, Khamaria, Jabalpur 482 005, Madhya Pradesh, India
E-mail: pcmishra_in@yahoo.com

MS received 5 October 2017; revised 21 February 2018; accepted 12 March 2018; published online 24 July 2018

Abstract. The occurrence of free radicals such as superoxide radical anion ($O_2^{\cdot-}$), hydroxyl radical ($OH^{\cdot}$), methoxy radical ($OCH_3^{\cdot}$) and nitrogen dioxide radical ($NO_2^{\cdot}$) inside living cells can be very hazardous as these radicals can modify structures and functions of different biomolecules. Both exogenous antioxidants taken as components of diet and endogenous enzyme antioxidants can scavenge $O_2^{\cdot-}$ separately. Mechanisms of scavenging $O_2^{\cdot-}$ by combinations of exogenous and endogenous enzyme antioxidants are not understood properly. In order to understand mechanisms of scavenging $O_2^{\cdot-}$, $OH^{\cdot}$, $OCH_3^{\cdot}$, and $NO_2^{\cdot}$ by allicin, and possible roles of superoxide dismutase (SOD) in scavenging $O_2^{\cdot-}$, density functional theory was employed. Marcus theory was also employed to study scavenging of $OH^{\cdot}$, $OCH_3^{\cdot}$ and $NO_2^{\cdot}$ by electron transfer. In order to find the most probable mechanisms of scavenging these radicals, different types of reactions such as one and two hydrogen atom transfer (HAT), single electron transfer (SET) and sequential proton loss electron transfer (SPLET) processes were investigated. It is found that allicin can scavenge $O_2^{\cdot-}$ *via* double hydrogen atom transfer catalyzed by Fe-SOD efficiently. Further, allicin can scavenge $OH^{\cdot}$ by SET, and $OCH_3^{\cdot}$ and $NO_2^{\cdot}$ by SPLET mechanisms most efficiently. Our results are in qualitative agreement with the available experimental data wherever these are available.

Keywords. Allicin; antioxidant; superoxide dismutase; radical scavenger; DFT study.

1. Introduction

During the normal cellular metabolism, the leakage and transfer of electrons to molecular oxygen gave rise to the formation of potentially damaging reactive superoxide radical anion ($O_2^{\cdot-}$).[1–3] Other reactive species such as hydroxyl radical ($OH^{\cdot}$), methoxy radical ($OCH_3^{\cdot}$), nitrogen dioxide radical ($NO_2^{\cdot}$), hydroperoxyl radical ($OOH^{\cdot}$) and carbonate radical anion ($CO_3^{\cdot-}$) *etc.*, can also be formed in cells following different mechanisms.[4–8] These reactive species interfere with the normal functioning of the living cells[9–13] and ultimately induce different pathological conditions.[14–16] Thus, protection of biological systems from damages caused by these free radicals is vital for the longevity of the cells. Fortunately, living systems are equipped with certain antioxidants that protect cells by converting the free radicals into unreactive forms. The intake of exogenous antioxidants as food supplements can also protect cells from free radical injuries by scavenging the free radicals. For example, recently curcumin,[17] ellagic acid,[18] 6-gingerol,[19] *etc.*, have been shown to scavenge hydroxyl radicals ($OH^{\cdot}$) efficiently by converting these to water (H_2O). Similarly, sulphoraphane[20] and ascorbic acid[21] have been found to scavenge $O_2^{\cdot-}$ by converting it to hydrogen peroxide (H_2O_2).

Recently, allicin, an extract of garlic, has been shown to possess antioxidant properties.[22] The antibacterial, antifungal and antiparasitic activities of garlic are also believed to be related to allicin. It should be mentioned

*For correspondence

Electronic supplementary material: The online version of this article (https://doi.org/10.1007/s12039-018-1509-1) contains supplementary material, which is available to authorized users.

that allicin is formed from alliin by alliinase enzyme[23,24] when garlic is crushed and it is also mainly responsible for its aroma.[25,26] Allicin permeates easily through the lipid membranes and readily interacts with thiol containing proteins.[27] Okada and co-workers[28] have recently evaluated the cumene and methyl linoleate derived peroxyl radical ($OOH^{\cdot}$) scavenging activity of allicin by using the HPLC technique in chlorobenzene. The rate constants involved in these reactions were found to be $2.6 \times 10^3 M^{-1} s^{-1}$ and $1.6 \times 10^5\ M^{-1} s^{-1}$, respectively. Lynett *et al.,*[29] have also observed allicin to scavenge $OOH^{\cdot}$ *via* the radical trapping mechanism. However, the $OH^{\cdot}$ radical scavenging activity of allicin is somewhat controversial. For example, Rabinkov and co-workers,[30] by using ESR technique, have observed a pronounced $OH^{\cdot}$ radical scavenging activity of allicin, whereas the study carried out by Chung[31] does not support it. Hence, it is necessary to examine $OH^{\cdot}$ radical scavenging ability of allicin to resolve the controversy. It is also desirable to find if allicin can also scavenge other reactive free radicals such as $O_2^{\cdot -}$, $OCH_3^{\cdot}$ and $NO_2^{\cdot}$.

It should be mentioned that the different superoxide dismutases (SODs) present in living systems can neutralize $O_2^{\cdot -}$ by converting it to molecular oxygen (Eq. 1) or to the comparatively less reactive molecule H_2O_2 (Eq. 2).[32,33] Thus, in the presence of SOD, $O_2^{\cdot -}$ is the precursor of formation of H_2O_2. These reactions mainly involve the metal centres (Ni, Mn, Fe, Cu or Zn) present at the active sites of the SODs.

$$O_2^{\cdot -} + Fe^{3+} \longrightarrow O_2 + Fe^{2+} \quad (1)$$

$$O_2^{\cdot -} + 2H^+ + e^- \longrightarrow H_2O_2 \quad (2)$$

Recently, using density functional theory (DFT), it has been shown that Fe-SOD catalyses scavenging of $O_2^{\cdot -}$ by sulforaphane[20] and ascorbic acid[21] following a single step two hydrogen atom transfer (HAT) mechanism. It is highly desirable to study if Fe-SOD can catalyze scavenging of $O_2^{\cdot -}$ by other natural antioxidants like allicin also since such studies would show if the catalytic mechanism involved in these reactions is general. Owing to the above-mentioned facts, DFT studies have been carried out here to understand $O_2^{\cdot -}$, $OH^{\cdot}$, $OCH_3^{\cdot}$ and $NO_2^{\cdot}$ scavenging activities of allicin in the absence and presence of Fe-SOD. In order to identify the most feasible pathways of these reactions, three different mechanisms, *i.e.*, hydrogen atom transfer (HAT), single electron transfer (SET), and sequential proton loss electron transfer (SPLET) processes have been investigated.

2. Computational methodology

The geometry of allicin was optimized using the M06-2X DFT functional[34,35] along with the 6-311+G(d) basis set in the gas phase. This is one of the best functionals to study molecular structures, properties and reactions.[34,35] The reactions of allicin with $OH^{\cdot}$, $OCH_3^{\cdot}$, $NO_2^{\cdot}$, and $O_2^{\cdot -}$ were studied by optimizing structures of the different reactants separately, transition states (TSs) and product complexes (PCs) at the same level of theory in the gas phase. When geometry optimization was performed placing $O_2^{\cdot -}$ near the various pairs of carbon sites of allicin in order to obtain different reactant complexes (RCs), the positions of $O_2^{\cdot -}$ got changed significantly making identification of RCs as involving the specific pairs of carbon sites impossible. Due to this reason, barrier energies were calculated with respect to the separate reactants. In order to study the reactions of $O_2^{\cdot -}$ with allicin in the presence of Fe-SOD, the model of Fe-SOD discussed earlier was employed.[20,21] In this model of Fe-SOD, three histidine rings bonded with a Fe^{3+} cation located at the centre is considered.[20,21] The structure of this model of Fe-SOD was also optimized at the above-mentioned level of theory in the gas phase.[20] A water molecule and a molecule of aspartic acid should also be considered as bound to the Fe cation according to the observed structure of Fe-SOD, but these were not included in the model for the sake of computational convenience hoping that the model would still reveal the important features of catalysis by the enzyme. To account for the solvent effect of the aqueous medium, single-point energy polarizable continuum model (PCM) calculations were performed employing its integral equation formalism.[36,37] In order to find charge distributions on various atoms of the reactants, TSs and PCs, natural bond orbital (NBO) analysis was performed.

The genuineness of all the optimized total energy minima in the gas phase was ensured by examining vibrational frequencies all of which were found to be real for the reactants and PCs. For each TSs, one vibrational frequency was found to be imaginary. As geometry optimization was not performed in an aqueous medium, zero-point energy and thermal energy corrections obtained in the gas phase were considered to be valid for the single point energies obtained in aqueous medium also. Rate constants involved in all radical scavenging reactions were calculated using Gibb's reaction barrier energies (Eq. 3) employing the thermal reaction rate constant equation (Eq. 4)[38] including tunnelling correction.

$$\Delta G^b = G_{TS} - G_{React} \quad (3)$$

$$k = \Gamma(T)(k_B T/h)\exp(-\Delta G^b/RT) \quad (4)$$

Here, ΔG^b, G_{TS} and G_{React} are Gibbs barrier energy of the reaction under consideration, Gibbs free energy of the transition state and the sum of Gibbs free energies of the reactants, respectively. $\Gamma(T)$ is the quantum mechanical tunnelling factor which was obtained considering an unsymmetric parabolic potential barrier using the method of Skodje and Truhlar.[39] This method to calculate tunnelling correction has been shown to provide accuracy that is comparable to that obtained by the

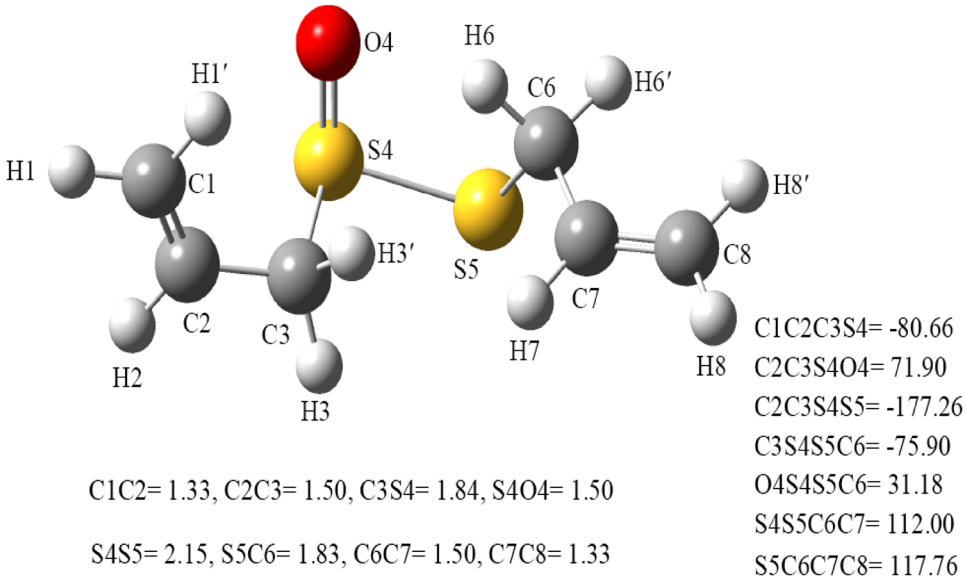

Figure 1. Optimized geometry of allicin, adopted atomic numbering scheme and some selected bond lengths (Å) and dihedral angles (Deg.).

WKB method.[39] Here, k_B is the Boltzmann constant, T is the absolute temperature (298.15 K), h is the Planck's constant and R is the gas constant. All the calculations were performed using the Windows version of the Gaussian09 suit of programs (G09W, Rev. B).[40] Optimized structures of the molecules and complexes were visualized using the Windows version of the GaussView (ver. 5.0) program.[41]

3. Results and Discussion

Atomic numbering scheme in allicin, its optimized geometry in the gas phase at the M06-2X/6-311+G(d) level of density functional theory and values of some selected geometrical parameters are given in Figure 1. As can be seen from this Figure 1, allicin has a thiosulphinate (R-S(O)-S-R, R=CH_2CHCH_2) functional group and two non-planar CH_2CHCH_2 groups are attached to each sulphur atom.

3.1 *Double hydrogen atom transfer to $O_2^{\cdot -}$ in the absence of Fe-SOD*

It is clear that transfer of an electron from $O_2^{\cdot -}$ to some other chemical species and transfer of one and two hydrogen atoms to it would convert it to the $OOH^{\cdot}$ group and H_2O_2. These mechanisms have recently been found to be operational when the exogenous antioxidants sulforaphane and ascorbic acid interact with $O_2^{\cdot -}$.[20,21] In order to examine if these mechanisms are also operational when allicin interacts with $O_2^{\cdot -}$, hydrogen atom transfer from neighboring carbon sites of allicin was considered. Double hydrogen atom transfer leading to the formation of H_2O_2 was found to take place only from the neighboring carbon sites. The neighboring sites of allicin from where pairs of hydrogen atoms were considered to be abstracted by superoxide radical anion are (C1,C2), (C2,C3), (C6,C7) and (C7,C8) (Figure 1). The double hydrogen abstraction process from the neighboring carbon sites occurs automatically and we do not have to make any extra provision for it, obviously as it keeps atomic valencies satisfied. Double hydrogen atom transfer from allicin in the absence of Fe-SOD can be expressed as shown in Equation 5:

$$\text{A-H}_n + O_2^{\cdot -} \xrightarrow{\Delta G_b} \text{A-H}_n - O_2^{\cdot -} \xrightarrow{\Delta G_r} \text{A} - \text{H}_{n-2} + H_2O_2 \quad (5)$$

where, the transition states, reactants and product complexes are located in the middle, left and right sides of the equation, respectively. A-H_n and A-H_{n-2} represent normal allicin and allicin minus two hydrogen atoms which have been transferred to $O_2^{\cdot -}$, respectively, and H_2O_2 is formed as a component of the product complexed with A-H_{n-2}. The (−2) negative charge on $O_2^{\cdot -}$ would be distributed to the different atoms in the product complex. Optimized geometries of the transition state and product complexes along with some bond lengths (Å) and imaginary frequencies (cm^{-1}) involved in the reactions are shown in Figure 2. The Gibbs barrier energy and released energy involved in double hydrogen atom transfer from each pair of sites in both the gas phase and aqueous medium are presented in Table 1.

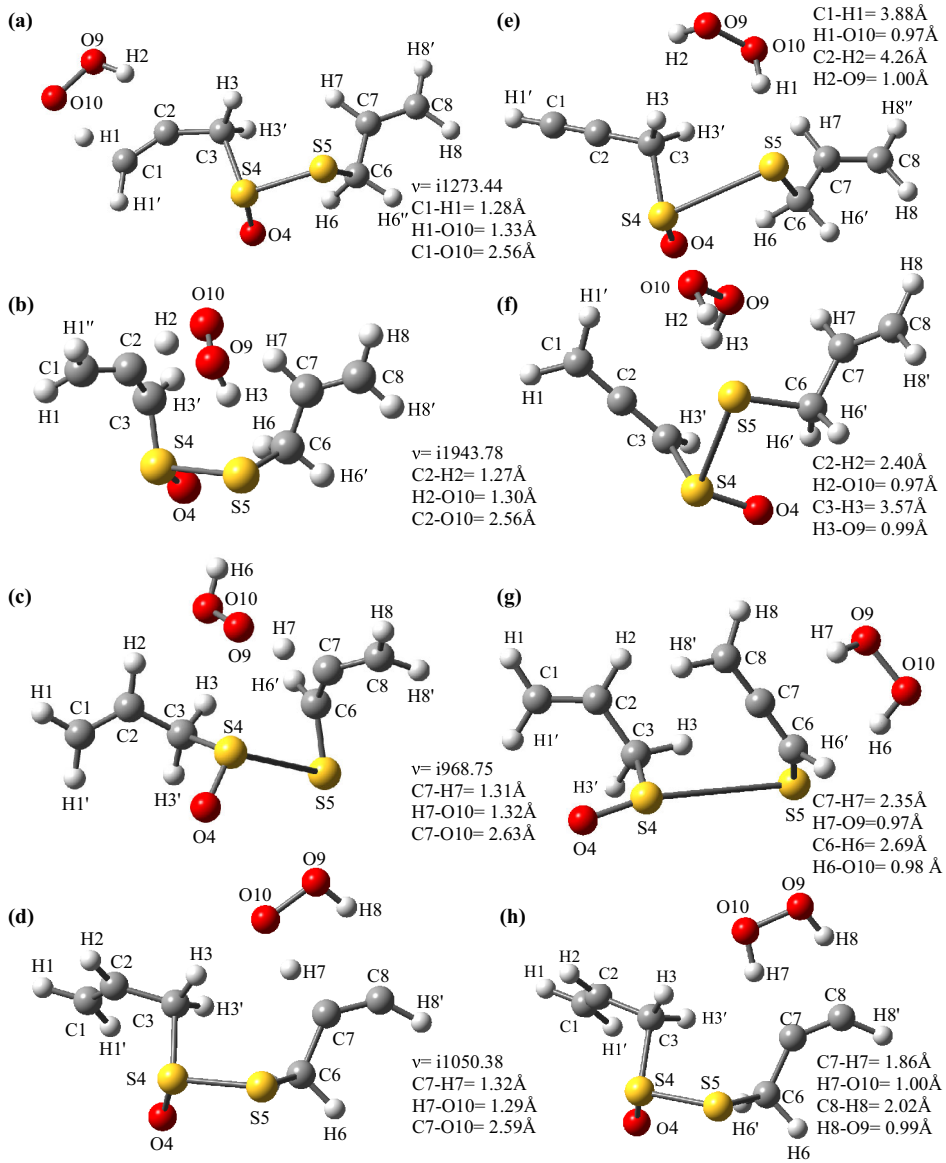

Figure 2. Optimized geometries of transition states (a–d) and corresponding product complexes (e–h) involved in single step double hydrogen atom transfer from the different pairs of neighboring sites of allicin to superoxide radical anion in the absence of Fe-SOD in gas phase.

Table 1. Barrier and released energies in terms of Gibbs (ΔG kcal/mol), enthalpy (ΔH kcal/mol) and entropy (ΔS kcal/mol-K) at 298.15K involved in double hydrogen atom transfer from different pairs of sites of allicin to $O_2^{\cdot-}$ in absence of Fe-SOD obtained at the M06-2X/6-311+G(d) level of density functional theory in gas phase and aqueous media.

Reaction sites	Barrier energy[a]			Released energy[a]		
	ΔG^b	ΔH^b	ΔS^b	ΔG^r	ΔH^r	ΔS^r
(C1,C2)	31.70 (54.34)	23.33 (46.00)	−0.03 (−0.03)	−42.94 (−38.65)	−42.20 (−37.91)	0.00 (0.00)
(C2,C3)	9.84 (40.58)	−0.60 (30.17)	−0.03 (−0.03)	−25.47 (−27.62)	−22.87 (−25.01)	0.01 (0.01)
(C6,C7)	−8.77 (20.56)	−15.36 (14.02)	−0.02 (−0.02)	−15.95 (−16.01)	−15.14 (−15.20)	0.00 (0.00)
(C7,C8)	35.34 (58.86)	25.27 (48.84)	−0.03 (−0.03)	−2.33 (−0.76)	−1.51 (1.57)	0.00 (0.00)

[a]Results obtained in aqueous media are given in parentheses.

In the absence of Fe-SOD, barrier energies involved in double hydrogen atom transfer from the (C1,C2), (C2,C3), (C6,C7) and (C7,C8) sites of allicin are 31.70, 9.84, −8.77 and 35.34 kcal/mol in gas phase, while in aqueous medium the corresponding barrier energies are 54.34, 40.58, 20.56 and 58.86 kcal/mol. These results reveal that in the gas phase, the double hydrogen abstraction barrier energies are much smaller than those in an aqueous medium, and barrier energies are enhanced by more than 20 kcal/mol in going from gas phase to aqueous medium each. Further, among the four pairs of sites, the barrier energy is least for the (C6,C7) pair of sites that are located in the neighborhood of the –S-S- group. In a previous study, the C6 site is reported to be the most reactive for the antioxidant action of allicin and thus the present calculated results in this context are supported by the previous ones.[28] Enhancement of barrier energy in going from the gas phase to the aqueous medium may be caused by the polarisation of the latter medium owing to the excess negative charge of superoxide radical anion due to which this species would be locally trapped and its reactivity reduced. Since for the three pairs of sites (C1,C2), (C2,C3) and (C6,C7), released energies (Table 1) are larger than the corresponding barrier energies in the gas phase, the corresponding reactions are exothermic. However, in going from the gas phase to the aqueous medium, released energies (Table 1) become less than the barrier energies, showing that the reactions have become endothermic. The reaction at the fourth pair of sites (C7,C8) is endothermic in both gas phase and an aqueous medium (Table 1).

The barrier and released energies involved in double hydrogen abstraction from pairs of sites of allicin by superoxide radical anion in the absence of Fe-SOD were computed in terms of enthalpy (kcal/mol) and entropy (kcal/mol-K) changes as given in Table 1. The contributions of entropy to the barrier and released energies are found to be negative, positive and significant at 298.15 K respectively. There is no significant difference between the gas phase and the aqueous phase values. Thus, entropy enhances the barrier heights for all pairs of sites in the absence of Fe-SOD; which means that entropy opposes the spontaneity of reactions to take place.

The results discussed above show that in the absence of Fe-SOD, scavenging of superoxide radical anion from biological media would not be likely to take place efficiently in both the gas phase and aqueous medium. We note that the results in aqueous medium would be much more relevant to the biological systems than those in the gas phase. Therefore, allicin would not serve as a good superoxide radical anion scavenger in the absence of an appropriate catalyst.

3.2 *Double hydrogen atom transfer in presence of Fe-SOD*

As mentioned in the previous section, the inability of allicin to scavenge $O_2^{\cdot -}$ in the absence of Fe-SOD appears to arise due to the trapping of $O_2^{\cdot -}$ in the aqueous medium that would be caused owing to the extra negative charge on it. When Fe-SOD is present, the positive charge on Fe^{+3} can neutralize the negative charge of $O_2^{\cdot -}$, thereby minimizing the trapping effect on its reactivity. The general scheme for double hydrogen atom transfer in presence of Fe-SOD will be similar to that presented in section 3.1 except that Fe-SOD will be present as a catalyst in this case (Equation 6).

$$\text{A-H}_n + O_2^{\cdot -} \xrightarrow[\text{Fe-SOD}]{\Delta G^b} \text{A-H}_n - O_2^{\cdot -} \xrightarrow[\text{Fe-SOD}]{\Delta G^r} \text{A} - \text{H}_{n-2} + H_2O_2 \quad (6)$$

Here, the transition state, reactants and products are located in the middle, left and right sides of the scheme and the different symbols have similar meanings as those discussed in the context of Equation 5. Consequent to the above reaction, Fe^{+3} is transformed to Fe^{+2}. It is known that Fe^{+2} can be transformed back to Fe^{+3} following the well-known Fenton reaction mechanism[42] that utilize the excess energy released (Table 2) due to the involvement of Fe-SOD as well as H_2O_2 producing $OH^{\cdot}$ and OH^-. However, we have not investigated this aspect here. The optimized structures of transition states involved in double hydrogen atom transfer from the (C1,C2), (C2,C3), (C6,C7) and (C7,C8) pair of sites of allicin along with some important bond lengths (Å) and imaginary frequencies are given in Figures 3 and 4, and the corresponding optimized structures of product complexes (PC) are presented in Figures S1 and S2 (in Supplementary Information). The Gibbs barrier and released energies involved in double hydrogen atom transfer from the (C1,C2), (C2,C3), (C6,C7) and (C7,C8) pairs of sites of allicin in both the gas phase and aqueous medium in presence of Fe-SOD are presented in Table 2.

The barrier and released energies involved in double hydrogen abstraction from pairs of sites of allicin by superoxide radical anion in the presence of Fe-SOD were also computed in terms of enthalpy (kcal/mol) and entropy (kcal/mol-K) changes and are given in Table 2. The contributions of entropy to the barrier and released energies are found to be positive and significant at 298.15 K, respectively. There is no significant difference between gas phase and aqueous phase values. Thus, the contributions of entropy to barrier energies are opposite while to the released energies, these are similar as discussed with regard to the results presented in Table 1.

Table 2. Barrier and released energies in terms of Gibbs (ΔG kcal/mol), enthalpy (ΔH kcal/mol) and entropy (Δ*S* kcal/mol-K) at 298.15K involved in double hydrogen atom transfer from different pairs of sites of allicin by $O_2^{\cdot-}$ in presence of Fe-SOD obtained at the M06-2X/6-311+G(d) level of density functional theory in gas phase and aqueous media.

Reaction sites	Barrier energy[a]			Released energy[a]		
	ΔG^b	ΔH^b	ΔS^b	ΔG^r	ΔH^r	ΔS^r
(C1,C2)	−31.06 (4.17)	−5.79 (29.50)	0.09 (0.09)	−14.75 (−26.27)	−14.03 (−25.54)	0.00 (0.00)
(C2,C3)	−24.84 (13.52)	−0.07 (38.29)	0.08 (0.08)	−17.27 (−38.37)	−11.61 (−32.71)	0.01 (0.01)
(C6,C7)	−37.66 (1.26)	−14.14 (24.78)	0.08 (0.08)	−11.79 (−27.07)	−8.65 (−23.93)	0.00 (0.00)
(C7,C8)	−25.41 (9.55)	2.21 (37.16)	0.09 (0.09)	−56.87 (−56.39)	−56.93 (−56.49)	0.00 (0.00)

[a]Results obtained in aqueous media are given in parentheses.

In the presence of Fe-SOD, in gas phase, the barrier energies involved in double hydrogen atom transfer to superoxide radical anion from the (C1,C2), (C2,C3), (C6,C7) and (C7,C8) pairs of sites of allicin are large negative *i.e.*, −31.06, −24.84, −37.66 and −25.41 kcal/mol (Table 2). Therefore, in the gas phase, the reactions at all the above pairs of sites of allicin would be barrier-less. A barrier energy is negative when its energy is less than the sum of energies of the reactants. In such a case, barrier and TS would not be observed, and only the product complex (PC) would be formed spontaneously when the reactants are brought together. In the aqueous medium, which is more relevant to the biological medium, the corresponding barrier energies are 4.17, 13.52, 1.26 and 9.55 kcal/mol, respectively (Table 2). Although in the aqueous medium, the barrier energies are much higher than those obtained in the gas phase, these are not too large to be overcome in the reactions under consideration. The reaction at the (C6,C7) pair of sites involves the lowest barrier energy in the aqueous medium, *i.e.*, 1.26 kcal/mol, and so, it would be the fastest. The reaction at the (C1,C2) pair of sites would also be quite fast since the corresponding barrier energy is moderate *i.e.*, 4.17 kcal/mol. In addition to this, it is also found that the inclusion of Fe-SOD in the above reaction makes the PC more stable than that found without Fe-SOD. This is because in the PC, one of the histidine molecules makes a strong hydrogen bond with the S=O group of allicin and the Fe cation is involved in a strong electrostatic interaction with H_2O_2. As a result, all the reactions would be appreciably exothermic. Thus, Fe-SOD would serve as a good catalyst in scavenging of $O_2^{\cdot-}$ by allicin. As Fe-SOD was also found to catalyze scavenging of $O_2^{\cdot-}$ by other antioxidants,[20,21] this phenomenon appears to be quite general. However, experimental evidence would be required to establish it.

Fe-SOD is a homodimer and the binding site of the superoxide radical anion on it is located near the dimer interface.[43] The enzyme has two regions that may control transit of substrate and product, one near the Fe cation and the other near the dimer interface.[43] Different classes of molecules have been found to act as inhibitors of different metal-SODs, *e.g.*, nitroprusside,[44] diethyldithiocarbamate[45,46] and benzo[g]phthalazine derivatives.[47,48] Many of these molecules are appreciably larger in size than allicin each and structures and sizes of the different classes of inhibitor molecules are also very different. Therefore, the modes of action of the different inhibitors are likely to be quite different which may also involve structural flexibility of the SOD near the active site as a common feature. Instead of binding with the active site metal, the different SOD inhibitors may act by other mechanisms, *e.g.*, hydrogen bonding with the protein.[48] The scavenging mechanism for $O_2^{\cdot-}$ proposed here does not require allicin to directly interact with the metal cation of Fe-SOD. Instead, allicin has only to remain in interaction with $O_2^{\cdot-}$ that is bound to the Fe cation. In this situation, the distances between the Fe cation and different sites of allicin can be appreciable.

The directly calculated distances between the Fe cation and the sites from where hydrogen atoms are abstracted in the product complexes shown in Figures S1 and S2 (Supplementary Information) lie in the range 4.63–5.91 Å while those at the transition states shown in Figures 3 and 4 lie in the range 3.92–5.37 Å. In the previous work on Mn-SOD,[49] there was water molecule also placed between the Mn cation and $O_2^{\cdot-}$, in accordance with the experimental observation.[50] In that case, the directly calculated distances between the Mn cation and the sites of dihydrolipoic acid from where hydrogen atoms were abstracted in the product complexes (transition states could not be located in that work[50]) were much larger, lying in the range 6.2–8.4 Å.[49] These distances show that for the catalytic action of Fe-SOD in double hydrogen abstraction by $O_2^{\cdot-}$ from allicin to take place, close interaction between the Fe cation and allicin is not necessary.

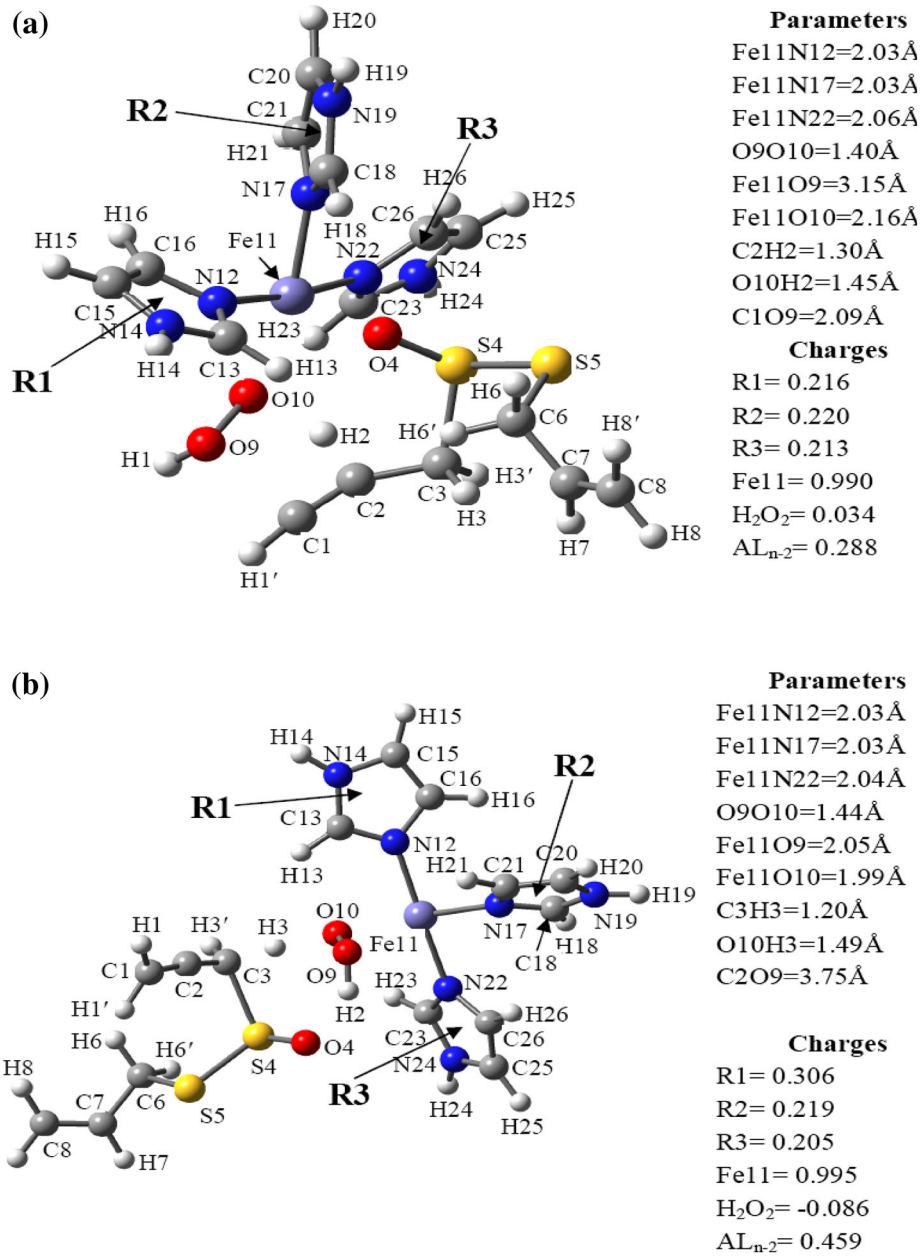

Figure 3. Optimized geometries of transition states ((a) TS1, (b) TS2)) involved in single step double hydrogen atom transfer from the (C1,C2) and (C2,C3) pairs of sites of allicin to superoxide radical anion in presence of Fe-SOD. Some important bond length (Å) and total net charges at the different rings (R1–R3), allicin (−2H), Fe cation and H_2O_2 are given.

3.3 *Optimized geometries and charge distributions*

Structures of the transition state and product complexes along with some important bond lengths (Å) as well net NBO charges at some selected atomic sites are presented in Figures 3 and 4, and in Figures S1 and S2 (Supplementary Information), respectively. Optimized values of the sets of dihedral angles Fe11N12C16H16 (ring 1), Fe11N17C21H21 (ring 2) and Fe11N22C26H26 (ring 3) in PC1, PC2, PC3 and PC4 are (7.49, 11.27, 9.98), (−2.09, 0.67, 6.42), (4.11, 1.84, −0.52) and (0.78, 7.93, 4.02) deg. while the corresponding dihedral angles in the absence of allicin (*i.e.*, in the complex of Fe-SOD with $O_2^{\cdot-}$) are (6.03, 1.47, 6.56), respectively. These values of dihedral angles show that only small reorientations of the histidine rings take place consequent to the reactions at the different pairs of sites of allicin. In other words, the orientations of the histidine rings are flexible only to small extents. It is noted that in the first three transition states (TS1, TS2 and TS3 in Figures 3(a), (b), 4(a)), out of the two hydrogen atoms to be abstracted by superoxide radical anion in presence of Fe-SOD, one hydrogen

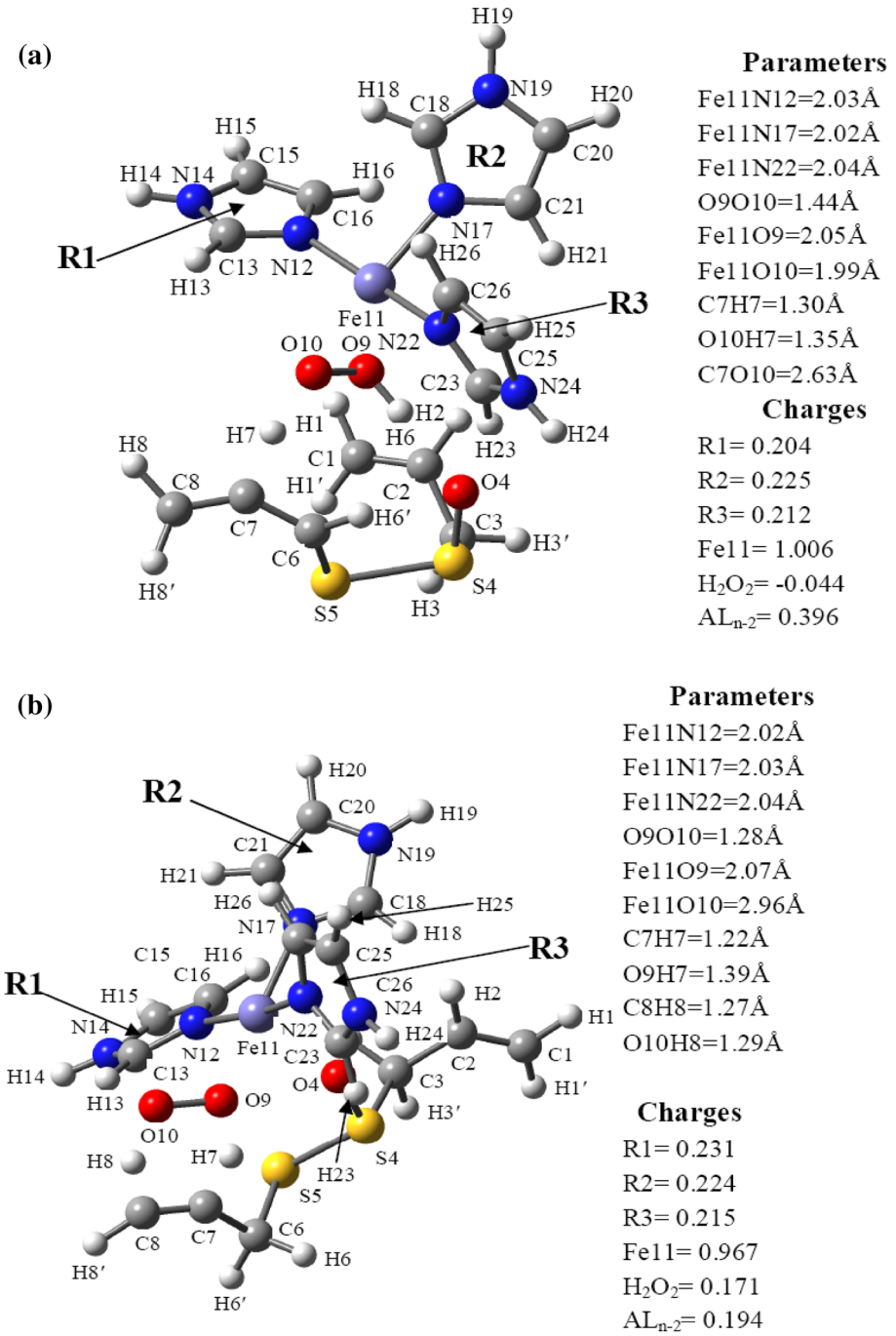

Figure 4. Optimized geometries of transition states ((a) TS3, (b) TS4)) involved in single step double hydrogen atom transfer from the (C6,C7) and (C7,C8) pairs of sites of allicin to superoxide radical anion in presence of Fe-SOD. Some important bond length (Å) and total net charges at the different rings (R1–R3), allicin (−2H), Fe cation and H_2O_2 are given.

atom (H1, H2 and H6) is abstracted first from allicin which gets attached to the O9 site of superoxide radical anion while the other hydrogen atoms (H2, H3 and H7) are still on the way between the O10 atom of superoxide radical anion and the carbon atom of allicin, *i.e.* C2, C3 and C7, respectively. Thus, although the two hydrogen atoms in these three transition states are not transferred simultaneously, transfer of both these is completed in a single reaction step in each case, and the transition state under consideration would correspond to transfer of the second hydrogen atom. At the transition state corresponding to double hydrogen atom transfer from the

(C7,C8) pair of sites of allicin, the two hydrogen atoms, on the basis of their locations, seem to be transferred only with a small delay (Figure 4(b)).

The NBO charges at the different atoms of allicin, all transition state complexes and the corresponding product complexes are presented in Tables S3–S11 (Supplementary Information). The total net NBO charges in the product complexes PC1, PC2 and PC3 (Tables S5, S7 and S9, in Supplementary Information) and those on the Fe site are found to lie between 1.116 and 1.238. In PC4 (Table S11, Supplementary Information), the Fe site carries a net NBO charge of 0.941. The different modified forms of allicin after double hydrogen atom transfer from its various pairs of sites carry net NBO charges lying between 0.053 and 0.238. The overall net NBO charges on the three histidine rings of Fe-SOD (Tables S4–S11, Supplementary Information) lie between 0.168 and 0.252. The NBO charges at the transition states presented in Tables S4, S6, S8 and S10 (Supplementary Information) are somewhat different from those in the corresponding product complexes. Thus, none of the components of product complexes, *i.e.,* modified allicin, H_2O_2 or Fe-SOD, carries a net negative charge. In other words, the extra negative charge of superoxide radical anion, consequent to product formation, is transferred only to the metal cation and no other component is involved in the reaction.

3.4 *Scavenging of $OH^{\cdot}$, $NO_2^{\cdot}$ and $OCH_3^{\cdot}$ by allicin*

We have investigated scavenging of $OH^{\cdot}$, $NO_2^{\cdot}$ and $OCH_3^{\cdot}$ by allicin considering the following two mechanisms: (i) Hydrogen atom transfer (HAT) and (ii) Single electron transfer (SET).

3.4a *Hydrogen atom transfer (HAT) mechanism*: Single hydrogen atom transfer to each of the $OH^{\cdot}$, $NO_2^{\cdot}$ and $OCH_3^{\cdot}$ free radicals can in principle take place from each of the six different sites C1, C2, C3, C6, C7 and C8 of allicin. The general scheme of single hydrogen atom transfer from any of these sites of allicin with n hydrogen atoms to $OH^{\cdot}$, $NO_2^{\cdot}$ or $OCH_3^{\cdot}$ can be given by Equation 7:

$$\text{A-H}_\text{n} + \text{R}^{\cdot} \xrightarrow{\Delta G^b} \text{A-H}_\text{n} - \text{R}^{\cdot} \xrightarrow{\Delta G^r} \text{A-H}^{\cdot}_{\text{n}-1} + \text{RH} \quad (7)$$

where, A-H_n and A-H_{n-1} represent allicin and its radical form having n and n−1 hydrogen atoms, respectively, and $R^{\cdot}$ is a free radical ($OH^{\cdot}$, $NO_2^{\cdot}$ or $OCH_3^{\cdot}$). The left, middle and right sides of the above reaction scheme show free reactants, transition state complex and product complex, respectively. The transition states, corresponding imaginary frequencies and product complexes including some important bond lengths involved in hydrogen atom transfer from the C1, C2, C3, C6, C7 and C8 sites of allicin to $OH^{\cdot}$, $NO_2^{\cdot}$ and $OCH_3^{\cdot}$ are presented in Figures 5–7, respectively, while the corresponding barrier and released energies in both gas phase and aqueous medium are presented in Table 3.

In the scavenging of $OH^{\cdot}$ in the aqueous medium, the C6 site of allicin involves least barrier energy (10.36 kcal/mol) and also, in this case, the product complex formed is most stable since the released energy is highest (38.41 kcal/mol) (Table 3). These results indicate that the C6 site is most favourable for HAT. The second least barrier energy involving the C7 site is 10.81 kcal/mol but in this case, the released energy is much smaller (14.71 kcal/mol) (Table 3). Therefore, hydrogen atom transfer from the C7 site would be much less favorable than from the C6 site. The C3 site involves a barrier energy of 11.46 kcal/mol for hydrogen atom transfer while the corresponding released energy is 32.65 kcal/mol. Therefore, the C3 site would also be less favored than the C6 site for the reaction. The barrier and released energies for hydrogen atom transfer from the C2 site are comparable and the same is true for the C8 site. Therefore, the product complexes involving hydrogen atom transfer from the C2 and C8 would not be quite stable. The C1 site involves a barrier energy of about 15.29 kcal/mol while the released energy is 13.33 kcal/mol (Table 3). Therefore, the reaction at this site would be endothermic and hence the product would not be stable. Thus, hydrogen atom transfer from the C6 site of allicin to $OH^{\cdot}$ would be the most likely process to take place.

In the scavenging of $NO_2^{\cdot}$ by allicin, reactions by the HAT mechanism at all the sites are associated with larger barrier energies (Table 3) than the corresponding released energies. Thus all these reactions are endothermic, and hence scavenging of $NO_2^{\cdot}$ by allicin through HAT from the different sites would not be favourable. In the case of scavenging of $OCH_3^{\cdot}$ by allicin by HAT, the lowest barrier energy in the aqueous medium is found for the C6 site but its value (16.54 kcal/mol) (Table 3) is quite large. The released energy, in this case, is 28.15 kcal/mol. Though the reaction at this site would be exothermic, the yield of the product complex would be low due to the large barrier energy. The reaction at the C3 site of allicin involves larger barrier and released energies (21.47 and 29.69 kcal/mol, respectively) than those at the C6 site. Therefore, the yield of the product complex for the C3 site would be smaller than even that at the C6 site. For the rest of the sites of allicin, *i.e.*, C1, C2, C7 and C8, the barrier energies are larger than the

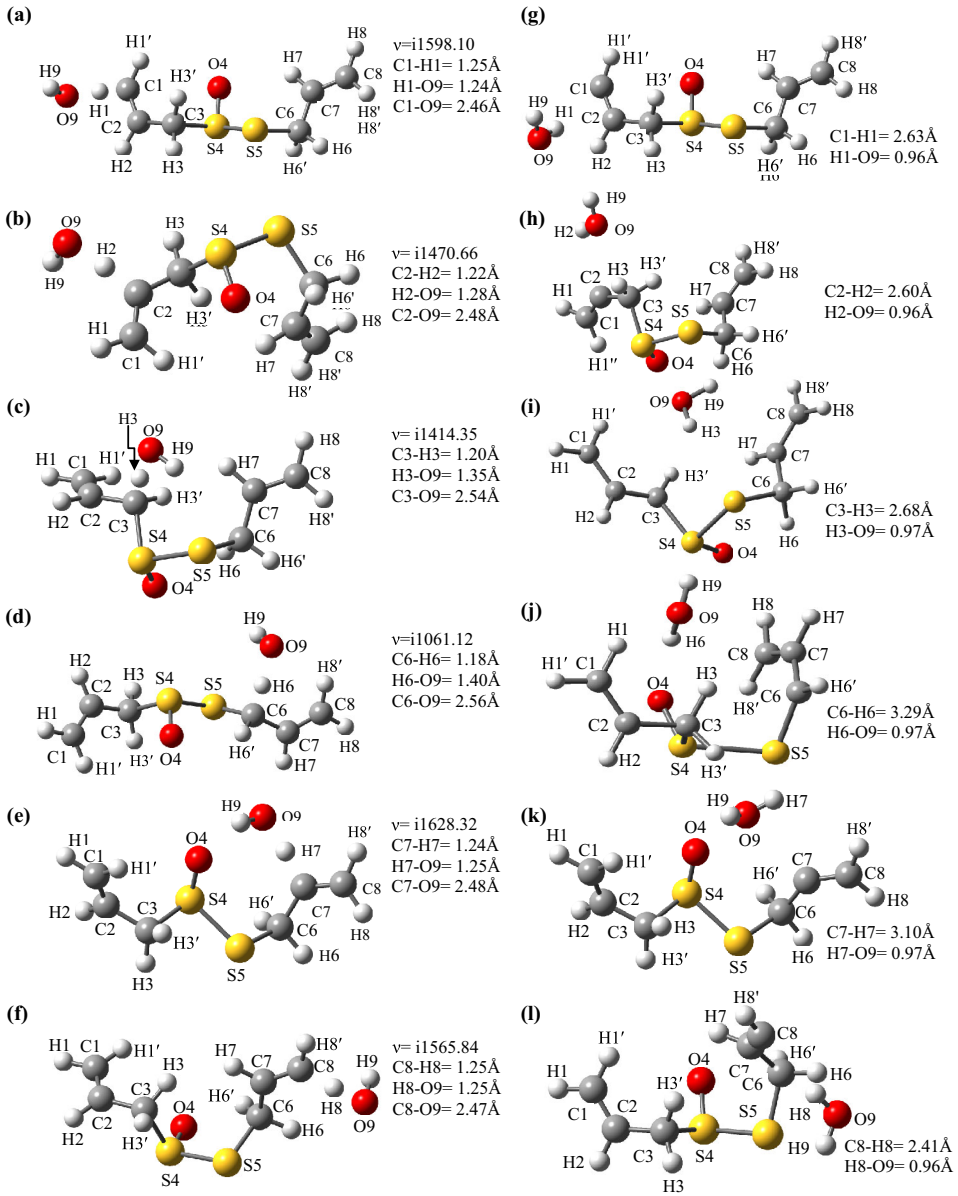

Figure 5. Optimized geometries of transition states (a–f, left side) and the corresponding product complexes (g–l, right side) involved in a hydrogen atom transfer from the different sites of allicin to a hydroxyl radical in the absence of Fe-SOD.

released energies. These results show that scavenging of $NO_2^{\cdot}$ $OCH_3^{\cdot}$ would also not take place efficiently by the HAT mechanism. Thus, the barrier and released energies presented in Table 3 reveal that out of the three radicals considered here, it is only $OH^{\cdot}$ that would be scavenged by allicin, and that too only with a low efficiency. The present results seem to resolve the controversy regarding the scavenging efficiency of allicin for hydroxyl radicals broadly supporting the results of Chung[31] in the sense that this molecule would not scavenge hydroxyl radicals efficiently.

The barrier and released energies involved in single hydrogen abstraction from the different sites of allicin by hydroxyl, nitrogen dioxide and methoxy radicals were also computed in terms of enthalpy (kcal/mol) and entropy (kcal/mol-K) changes and are given in Tables S1 and S2 (Supplementary Information). The contributions of entropy to the barrier and released energies are similar as discussed with regard to the results presented in Table 1 and, so, would have similar implications.

3.4b *Single electron transfer and sequential proton loss electron transfer*: Electron transfer is also an important mechanism to scavenge free radicals by reducing and modifying them to non-reactive forms. In order to examine if allicin can scavenge different free radicals by the single electron transfer (SET) and

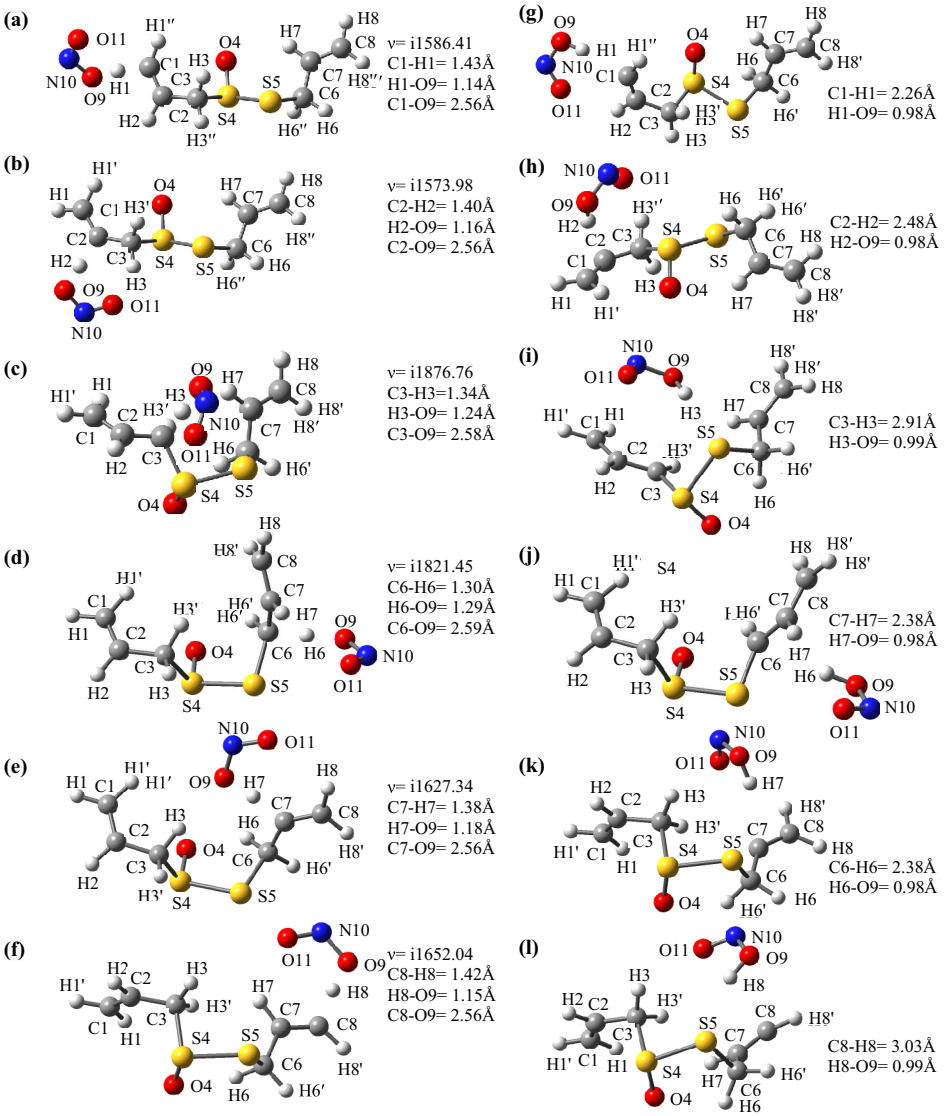

Figure 6. Optimized geometries of transition states (a–f, left side) and the corresponding product complexes (g–l, right side) involved in a hydrogen atom transfer from the different sites of allicin to a nitrogen dioxide radical in the absence of Fe-SOD.

sequential proton loss electron transfer (SPLET) mechanisms, the Marcus theory was applied in an aqueous medium.[51,52] According to this theory, the electron transfer barrier energy (ΔG^{b}_{ET}) (Eq. 8) is obtained as follows.

$$\Delta G^{b}_{ET} = \frac{\lambda}{4}\left(1 + \frac{\Delta G^{0}_{ET}}{\lambda}\right)^{2} \quad (8)$$

ΔG^{0}_{ET} = G1 − G2, where G1 = Sum of Gibbs energies of products (*e.g.*, $A^{+\cdot}$+OH^{-}); G2 = Sum of Gibbs energies of the reactants (*e.g.*, A + $OH^{\cdot}$). ΔG^{0}_{ET} and λ are Gibbs energy of the reaction and reorganization energy respectively. λ can be obtained using the approach (Eq. 9) adopted by Nelsen and co-workers as follows:[53,54]

$$\lambda = \Delta E^{0}_{ET} - \Delta G^{0}_{ET} \quad (9)$$

where, ΔE^{0}_{ET} is the vertical Gibbs energy difference between the reactants and products. This barrier energy can be used to obtain the electron transfer rate constant employing the transition state theory. The calculated barrier energies involved in single electron transfer from neutral allicin and allicin anion obtained by electron attachment to $OH^{\cdot}$, $NO_2^{\cdot}$ and $OCH_3^{\cdot}$ are presented in Table 4.

The results presented in this table reveal that electron transfer from neutral allicin to $OH^{\cdot}$, $NO_2^{\cdot}$ and $OCH_3^{\cdot}$ would practically not occur due to large barrier energies. In other words, neutral allicin cannot scavenge $OH^{\cdot}$, $NO_2^{\cdot}$ and $OCH_3^{\cdot}$ by the electron transfer mechanism. However, electron transfer from anionic allicin obtained by electron attachment to the radicals involve very small

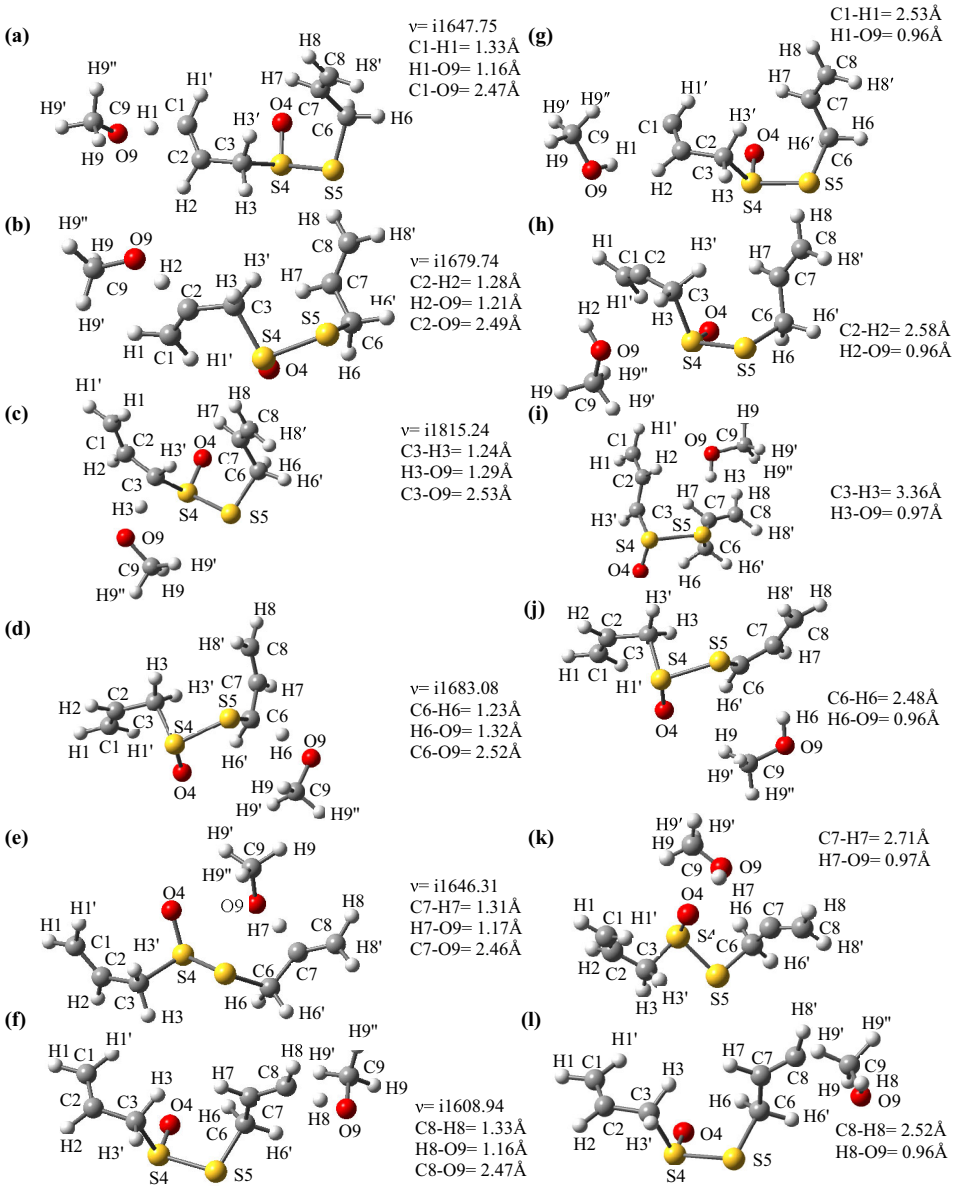

Figure 7. Optimized geometries of transition states (a–f, left side) and the corresponding product complexes (g–l, right side) involved in a hydrogen atom transfer from the different sites of allicin to a methoxy radical in the absence of Fe-SOD.

barrier energies, *i.e.*, 0.24, 2.61 and 3.11 kcal/mol for $OH^{\cdot}$, $NO_2^{\cdot}$ and $OCH_3^{\cdot}$, respectively (Table 4). Therefore, allicin anion obtained by electron attachment would scavenge $OH^{\cdot}$, $NO_2^{\cdot}$ and $OCH_3^{\cdot}$ very efficiently by the electron transfer mechanism.

Another possible mechanism of electron transfer is that of sequential proton loss electron transfer (SPLET).[55–57] In order to study electron transfer by the SPLET mechanism, a proton is considered to be removed from each of the different carbon centres (C1 to C3 and C6 to C8) of allicin producing six deprotonated species ($A(-H^+)^-$). Subsequently, an electron is considered to be transferred from each of the $A(-H^+)^-$ species to the different free radicals. Barrier energies involved in SPLET for the different sites of allicin to $OH^{\cdot}$, $NO_2^{\cdot}$ and $OCH_3^{\cdot}$ thus obtained are presented in Table 5. These results reveal that the SPLET mechanism for $OH^{\cdot}$ involves the lowest barrier energy (1.23 kcal/mol) for the C3 site while the highest SPLET barrier energy (19.94 kcal/mol) corresponds to the C6 site. However, for $NO_2^{\cdot}$ and $OCH_3^{\cdot}$, the SPLET barrier energies are negligible (not exceeding 0.2 kcal/mol) for all the sites of allicin, except for the C3 site for which also the barrier energies are quite low but significant (not

Table 3. Gibbs barrier (ΔG^b) and released (ΔG^r) energies (kcal/mol) at 298.15 K involved in hydrogen atom transfer from different sites of allicin to $OH^{\cdot}$, $NO_2^{\cdot}$ and $OCH_3^{\cdot}$ obtained at the M06-2X/6-311+G(d) level of density functional theory in gas phase and aqueous media.[a]

Sl. No.	Reaction site	$OH^{\cdot}$		$NO_2^{\cdot}$		$OCH_3^{\cdot}$	
		ΔG^b	ΔG^r	ΔG^b	ΔG^r	ΔG^b	ΔG^r
1	C1	15.11 (15.29)	−13.16 (−13.33)	44.76 (44.04)	−5.17 (−5.06)	26.03 (27.27)	−8.60 (−8.27)
2	C2	13.02 (14.69)	−16.46 (−16.15)	39.30 (39.26)	−4.46 (−4.15)	23.80 (26.44)	−12.73 (−12.42)
3	C3	9.55 (11.46)	−33.46 (−32.65)	33.56 (33.39)	−20.11 (−19.98)	20.01 (21.47)	−29.11 (−50.69)
4	C6	9.01 (10.36)	−40.54 (−38.41)	29.75 (29.94)	−18.57 (−18.60)	14.78 (16.54)	−27.24 (−28.12)
5	C7	10.19 (10.81)	−15.22 (−14.71)	40.59 (41.40)	−7.46 (−7.92)	22.84 (23.42)	−12.81 (−12.08)
6	C8	14.79 (15.59)	−13.91 (−17.74)	42.94 (42.66)	−4.85 (−4.24)	24.66 (25.63)	−7.61 (−8.37)

[a]Results obtained in aqueous media are given in parentheses.

Table 4. Gibbs barrier (ΔG^b_{ET}) energies (kcal/mol) at 298.15 K involved in direct electron transfer from allicin (AL) and allicin anion (AL^-) to $OH^{\cdot}$, $NO_2^{\cdot}$ and $OCH_3^{\cdot}$ obtained at the M06-2X/6-311+G(d) level of density functional theory in aqueous media.

Sl. No.	Electron donor	Electron acceptor		
		$OH^{\cdot}$	$NO_2^{\cdot}$	$OCH_3^{\cdot}$
1	AL	71.91	35.35	99.20
2	AL^-	0.24	2.61	3.11

Table 5. Gibbs barrier (ΔG^b_{ET}) energies (kcal/mol) at 298.15 K involved in sequential proton loss electron transfer (SPLET) involving different sites of allicin to $OH^{\cdot}$, $NO_2^{\cdot}$ and $OCH_3^{\cdot}$ obtained at the M06-2X/6-311+G(d) level of density functional theory in aqueous media.

Sl. No.	Deprotonation site	Electron acceptor		
		$OH^{\cdot}$	$NO_2^{\cdot}$	$OCH_3^{\cdot}$
1	C1	6.11	0.04	0.00
2	C2	4.97	0.10	0.03
3	C3	1.23	1.77	4.06
4	C6	19.94	0.11	0.04
5	C7	7.05	0.00	0.09
6	C8	9.88	0.00	0.18

exceeding 4.06 kcal/mol). Thus, we find that the Gibbs barrier energies for electron transfer by the SET mechanism from anionic allicin or by the SPLET mechanism from allicin to any of the $NO_2^{\cdot}$ and $OCH_3^{\cdot}$ radicals are quite small while those obtained considering the SPLET mechanism to $OH^{\cdot}$ (except for the C3 site) are appreciably larger (Tables 4 and 5).

3.5 *Rate constants*

The calculated thermal rate constants k for double hydrogen atom transfer to superoxide radical anion ($O_2^{\cdot -}$) from the different pairs of sites of allicin in the absence and presence of Fe-SOD corresponding to barrier energies given in Tables 1 and 2 including tunneling corrections are presented in Table 6 while the values of the corresponding tunneling corrections Γ(T) only are presented in Table S12 (Supplementary Information). Tunnelling correction is significant for the reaction at the (C2,C3) pair of sites in an aqueous medium in the absence of Fe-SOD. The results presented in Table 6 reveal that in the absence of Fe-SOD, the highest rate constants corresponds to the (C6,C7) pair of sites among all the four pairs of sites ((C1,C2), (C2,C3), (C6,C7) and (C7,C8)) of allicin in both the gas phase and aqueous medium. Except for the (C6,C7) pair of sites of allicin, in the absence of Fe-SOD in an aqueous medium, the different thermal rate constants are $\sim 10^{-13}$ M^{-1} s^{-1} or less while for the (C6,C7) pair of sites, the corresponding thermal rate constant is $\sim 10^{-3}$ M^{-1} s^{-1}. It implies that in the absence of Fe-SOD, allicin would be a very poor scavenger of superoxide radical anion. However, when Fe-SOD is present, it catalyses reactions at all the four pairs of sites, the catalytic action for the (C6,C7) pair of sites being most prominent, and the thermal rate constant at this pair of sites in the aqueous medium is highly enhanced *i.e.* to 10^{12} M^{-1} s^{-1} (Table 6). Thermal rate

Table 6. Thermal rate constants (k) ($M^{-1}\ s^{-1}$) at 298.15 K for double hydrogen atom transfer to superoxide radical anion ($O_2^{\cdot -}$) from the different pairs of sites of allicin in absence and presence of Fe-SOD obtained at the M06-2X/6-311+G(d) level of density functional theory in gas phase and aqueous media.[a]

Sl. No.	Reaction sites	Without Fe-SOD	With Fe-SOD
1	(C1,C2)	8.94×10^{-11} (2.22×10^{-27})	6.21×10^{12} (1.06×10^{10})
2	(C2,C3)	1.87×10^{6} (4.97×10^{-17})	6.21×10^{12} (8.43×10^{2})
3	(C6,C7)	6.21×10^{12} (8.94×10^{-3})	6.21×10^{12} (1.65×10^{12})
4	(C7,C8)	1.54×10^{-13} (8.63×10^{-31})	6.21×10^{12} (1.70×10^{6})

[a]Thermal rate constants (k) in aqueous media are given in parentheses.

Table 7. Thermal rate constants (k) ($M^{-1}\ s^{-1}$) at 298.15 K for hydrogen atom transfer from the different sites (C1, C2, C3, C6, C7 and C8) of allicin to $OH^{\cdot}$, $NO_2^{\cdot}$ and $OCH_3^{\cdot}$ obtained at the M06-2X/6-311+G(d) level of theory in gas phase and aqueous media.

Sl. No.	Reaction site[a]	$OH^{\cdot}$	$NO_2^{\cdot}$	$OCH_3^{\cdot}$
1	C1	1.79×10^{2} (1.31×10^{2})	3.15×10^{-20} (1.06×10^{-19})	1.82×10^{-6} (2.24×10^{-7})
2	C2	5.41×10^{3} (3.22×10^{2})	3.15×10^{-16} (3.37×10^{-16})	8.08×10^{-5} (9.36×10^{-7})
3	C3	1.80×10^{6} (7.15×10^{4})	6.63×10^{-12} (8.84×10^{-12})	5.47×10^{-2} (3.40×10^{-19})
4	C6	3.20×10^{6} (3.26×10^{5})	3.95×10^{-9} (2.86×10^{-9})	3.35×10^{2} (1.71×10^{1})
5	C7	7.42×10^{5} (2.60×10^{5})	3.74×10^{-17} (9.53×10^{-18})	3.97×10^{-4} (1.49×10^{-4})
6	C8	2.97×10^{2} (7.68×10^{1})	7.22×10^{-19} (1.16×10^{-18})	1.78×10^{-5} (3.45×10^{-6})

[a]Thermal rate constants (k) in aqueous media are given in parentheses.

constants k ($M^{-1}\ s^{-1}$) including tunnelling corrections for hydrogen atom transfer to $OH^{\cdot}$, $NO_2^{\cdot}$ and $OCH_3^{\cdot}$ from the six different sites (C1, C2, C3, C6, C7 and C8) of allicin are presented in Table 7 while the values of corresponding tunnelling corrections Γ(T) only are presented in Table S13 (Supplementary information). Tunnelling corrections are appreciable for the reaction with $NO_2^{\cdot}$ at the C3 site in both gas phase and an aqueous medium. These rate constants were calculated using the corresponding Gibbs barrier energies presented in Table 3. Both the thermal rate constants for scavenging $OH^{\cdot}$ by hydrogen atom transfer from the C6 and C7 sites of allicin in an aqueous medium are about $10^5 M^{-1}\ s^{-1}$ (Table 7).

For all the other four sites involved in hydrogen atom transfer to $OH^{\cdot}$ in an aqueous medium, the thermal rate constants lie in the range 10^1 to $10^4\ M^{-1}\ s^{-1}$. For hydrogen atom transfer to $NO_2^{\cdot}$ in aqueous medium from all the six sites (C1, C2, C3, C6, C7 and C8) of allicin, the thermal rate constants are found to be very small (10^{-19} to $10^{-9}\ M^{-1}s^{-1}$), and for hydrogen atom transfer to $OCH_3^{\cdot}$ in aqueous medium also, except for the C6 site, the thermal rate constants lie in the range 10^{-19} to $10^{-6}\ M^{-1}s^{-1}$. For hydrogen atom transfer to $OCH_3^{\cdot}$ from the C6 site of allicin, the rate constant in the aqueous medium is $10^1\ M^{-1}s^{-1}$. The thermal rate constants in the gas phase are also qualitatively similar to those in an aqueous medium (Table 7). The experimental rate constant obtained by hydrogen abstraction by hydroperoxyl radicals was found to be of the order of $10^7\ M^{-1}\ s^{-1}$ which is 10^2 times larger than that of hydroxyl radical obtained in the present study. These results show that in both gas phase and an aqueous medium, allicin would exhibit a poor efficiency to scavenge $OH^{\cdot}$ than that for $OOH^{\cdot}$ by the HAT mechanism while it would almost not scavenge $NO_2^{\cdot}$ and $OCH_3^{\cdot}$ by the same mechanism.

As the Gibbs barrier energies for SET from neutral allicin to the radicals are very high (Table 4), the corresponding thermal rate constants are very small ($\sim 10^{-13}\ M^{-1}\ s^{-1}$ or smaller). Therefore, electron transfer under consideration would practically not take place. However, as the barrier energies for SET from the anion of allicin are quite small, the corresponding rate constants are quite large ($\sim 10^{11}$ to $\sim 10^{12}\ M^{-1}\ s^{-1}$). Rabinkov *et al.*[30] have observed a rate constant of $\sim 10^9 M^{-1}\ s^{-1}$ for scavenging of OH radicals by allicin experimentally using the ESR technique. Our calculated rate constant ($\sim 10^{11} M^{-1}\ s^{-1}$) is in a qualitative agreement with that value.[30] The difference in the calculated and observed rate constants may be ascribed to the different reaction environments in which these studies were performed. These results show that allicin anion would

serve as an efficient scavenger of $OH^{\cdot}$, $NO_2^{\cdot}$ and $OCH_3^{\cdot}$ radicals by the SET mechanism. The Gibbs barrier energies involved in the SPLET mechanism between allicin anion and $NO_2^{\cdot}$ or $OCH_3^{\cdot}$ radical (Table 5) show that electron transfer by this mechanism would also occur very efficiently (rate constants $\sim 10^{10}$ to $10^{12}\ M^{-1}\ s^{-1}$) while for the OH radical the corresponding process would be comparatively much slower (rate constants $\sim 10^{-2}\ M^{-1}\ s^{-1}$ for the C6 site and $\sim 10^{5}$ to $10^{11}\ M^{-1}\ s^{-1}$ for the other sites).

4. Conclusions

The present study of scavenging of $O_2^{\cdot -}$, $OH^{\cdot}$, $NO_2^{\cdot}$ and $OCH_3^{\cdot}$ in aqueous or biological media leads us to the following conclusions. In the absence of Fe-SOD, double hydrogen atom transfer from any of the four pairs of sites of allicin to $O_2^{\cdot -}$ cannot occur efficiently due to large barrier energies in an aqueous medium (>20 kcal/mol). Therefore, allicin would not serve as an efficient $O_2^{\cdot -}$ scavenger without the involvement of a catalyst. In presence of Fe-SOD, in aqueous medium, double hydrogen atom transfer to $O_2^{\cdot -}$ from each of the four pairs of sites of allicin would occur with smaller barrier energies lying in the range 1.26–13.5 kcal/mol, those corresponding to two pairs of sites being quite small (1.26 and 4.17 kcal/mol). Thus, Fe-SOD catalyses scavenging of $O_2^{\cdot -}$ by allicin efficiently. The present study appears to resolve the controversy regarding the scavenging efficiency of allicin for $OH^{\cdot}$, broadly supporting the results that allicin would not scavenge $OH^{\cdot}$ efficiently. Further, it is found that scavenging of $NO_2^{\cdot}$ and $OCH_3^{\cdot}$ radicals by allicin would practically be forbidden due to large barrier energies. Scavenging of $OH^{\cdot}$, $NO_2^{\cdot}$ and $OCH_3^{\cdot}$ by single electron transfer (SET) from neutral allicin would also be almost forbidden. On the contrary, scavenging of $NO_2^{\cdot}$ and $OCH_3^{\cdot}$ would occur very efficiently by sequential proton loss electron transfer (SPLET). However, scavenging of $OH^{\cdot}$ by SPLET would occur only with a moderate efficiency. Scavenging of all the three radicals would occur efficiently by SET from allicin anion.

Supplementary Information (SI)

Optimized geometries of the product complexes obtained by double hydrogen atom transfer from the (C1,C2), (C2,C3), (C6,C7) and (C7,C8) pairs of sites of allicin to superoxide radical anion in presence of Fe-SOD are presented as Supplementary Information in Figures S1 and S2, respectively. Barrier and released energies in terms of enthalpy and entropy corresponding to Table 3 are given in Tables S1 and S2, respectively. NBO charges at different atoms of allicin (Table S3), different transition states and product complexes involved in double hydrogen atom transfer are given in Tables S4–S11, respectively. Imaginary frequencies (cm^{-1}) and tunneling coefficients Γ(T) for double hydrogen atom transfer to superoxide radical anion from the different pairs of sites ((C1,C2), (C2,C3), (C6,C7) and (C7,C8)) of allicin in gas phase obtained at the M06-2X/6-311+G(d) level of theory in the absence and presence of Fe-SOD are given in Tables S12 and S13, respectively. Supplementary Information is available at www.ias.ac.in/chemsci.

Acknowledgements

One of the authors (PCM) is thankful to the National Academy of Sciences, India (NASI) for the award of a Senior Scientist Fellowship.

References

1. Fridovich I 1978 The biology of oxygen radicals *Science* **201** 875
2. Halliwell B and Gutteridge J M C 1984 Oxygen toxicity, oxygen radicals, transition metals and disease *Biochem. J.* **219**
3. Jena N R 2012 DNA damage by reactive species: Mechanisms, mutation and repair *J. Biosci.* **37** 503
4. Turrens J F 2003 Mitochondrial formation of reactive oxygen species *J. Physiol.* **552** 335
5. Beckman J S and Koppenol W H 1996 Nitric oxide, superoxide, and peroxynitrite: the good, the bad, and ugly *Am. J. Physiol.* **271** C1424
6. Radi R, Cassina A, Hodara R, Quijano C and Castro L 2002 Peroxynitrite reactions and formation in mitochondria *Free Rad. Biol. Med.* **33** 1451
7. Usmar V D and Halliwell B 1996 Blood radicals: reactive nitrogen species, reactive oxygen species, transition metal ions, and the vascular system *Pharm. Res.* **13** 649
8. Pryor W A 1986 Oxy-radicals and related species: their formation, lifetimes, and reactions *Annu. Rev. Physiol.* **48** 657
9. Wiseman H and Halliwell B 1996 Damage to DNA by reactive oxygen and nitrogen species: role in inflammatory disease and progression to cancer *J. Biochem.* **313** 17
10. Marnett L J 2000 Oxyradicals and DNA damage *Carcinogenesis* **21** 361
11. Hussain S P, Hofseth L J and Harris C C 2003 Radical causes of cancer *Nat. Rev. Cancer* **3** 276
12. Jena N R and Mishra P C 2005 Mechanisms of formation of 8-Oxoguanine due to reactions of one and two $OH^{\cdot}$ radicals and the H_2O_2 molecule with guanine: A quantum computational study *J. Phys. Chem. B* **109** 14205
13. Jena N R and Mishra P C 2012 Formation of ring-opened and rearranged products of guanine: Mechanisms and biological significance *Free Rad. Biol.* **53** 81
14. Simons J 2006 How do low-energy (0.1–2 eV) electrons cause DNA-strand breaks? *Acc. Chem. Res.* **39** 772
15. Mishina Y, Duguid E M and He C 2006 Direct reversal of DNA alkylation damage *Chem. Rev.* **106** 215
16. Neeley W L and Essigmann J M 2006 Mechanisms of formation, genotoxicity, and mutation of guanine oxidation products *Chem. Res. Toxicol.* **19** 491

17. Agnihotri N and Mishra P C 2011 Scavenging mechanism of curcumin toward the hydroxyl radical: a theoretical study of reactions producing ferulic acid and vanillin *J. Phys. Chem. A* **115** 14221
18. Tiwari M K and Mishra P C 2013 Modeling the scavenging activity of ellagic acid and its methyl derivatives towards hydroxyl, methoxy, and nitrogen dioxide radicals *J. Mol. Model.* **19** 5445
19. Tiwari M K and Mishra P C 2016 Anti-oxidant activity of 6-gingerol as a hydroxyl radical scavenger by hydrogen atom transfer, radical addition and electron transfer mechanisms *J. Chem. Sci.* **128** 1199
20. Prasad A K and Mishra P C 2015 Mechanism of action of sulforaphane as a superoxide radical anion and hydrogen peroxide scavenger by double hydrogen transfer: A model for iron superoxide dismutase *J. Phys. Chem. B 119* 7825
21. Tiwari M K and Mishra P C 2016 Catalytic role of iron-superoxide dismutase in hydrogen abstraction by super oxide radical anion from ascorbic acid *RSC Adv.* **6** 86650
22. Prasad K, Laxdal V A, Yu M and Raney B L 1995 Antioxidant activity of allicin, an active principle in garlic *Mol. Cell Biochem.* **148** 183
23. Lawson L D and Gardner C D 2005 Composition, stability, and bioavailability of garlic products used in a clinical trial *J. Agric. Food Chem.* **53** 6254
24. Xiao H and Parkin K L 2002 Antioxidant functions of selected allium thiosulfinates and S-alk(en)yl-L-cysteine sulfoxides *J. Agric. Food Chem.* **50** 2488
25. Block E 1992 The organosulfur chemistry of the genus allium-implications for the organic chemistry sulfur *Angew. Chem. Int. Edit. Engl.* **31** 1135
26. Block E 1985 The chemistry of garlic and onions *Sci. Am.* **252** 114
27. Miron T, Rabinkov A, Mirelman D, Wilchek M and Weiner L 2000 The mode of action of allicin: its ready permeability through phospholipid membranes may contribute to its biological activity *Biochim. Biophys. Acta* **1463** 20
28. Okada Y, Tanaka K, Sato E and Okajima H 2006 Kinetic and mechanistic studies of allicin as an antioxidant *Org. Biomol. Chem.* **4** 4113
29. Lynett P T, Butts K, Vaidya, V, Garrett G E and Pratt D A 2011 The mechanism of radical-trapping antioxidant activity of plant-derived thiosulfinates *Org. Biomol. Chem.* **9** 3320
30. Rabinkov A, Miron T, Konstantinovski L, Wilchek, M, Mirelman, D and Weiner L 1998 The mode of action of allicin: trapping of radicals and interaction with thiol containing proteins *Biochim. Biophys. Acta* **1379** 233
31. Chung L Y 2006 The antioxidant properties of garlic compounds: allyl cysteine, alliin, allicin, and allyl disulfide *J. Med. Food.* **9** 205
32. Fridovich I 1995 Superoxide radical and superoxide dismutases *Annu. Rev. Biochem.* **64** 97
33. Flint D H, Tuminello J F and Emptage M H 1993 The inactivation of Fe-S cluster containing hydro-lyases by superoxide *J. Biol. Chem.* **268** 22369
34. Zhao Y and Truhlar D G 2011 Applications and validations of the Minnesota density functional *Chem. Phys. Lett.* **502** 1
35. Zhao Y and Truhlar D G 2008 Exploring the limit of accuracy of the global hybrid meta density functional for main group thermochemistry, kinetics, and noncovalent interactions *J. Chem. Theory Comput.* **4** 1849
36. Miertus S, Scrocco E and Tomasi J 1981 Electrostatic interaction of a solute with a continuum. A direct utilization of Ab-Initio molecular potentials for the prevision of solvent effects *Chem. Phys.* **55** 117
37. Miertus S and Tomasi J 1982 Approximate evaluations of the electrostatic free energy and internal energy changes in solution processes *Chem. Phys.* **65** 239
38. Laidler K J 2004 In *Chemical Kinetics* 3rd edn. (Pearson Education (Singapore) Pte Ltd, Indian Branch, Patparganj, Delhi)
39. Skodje R T and Truhlar D G 1981 Parabolic tunnelling calculations *J. Phys. Chem.* **34** 624
40. Frisch M J, Trucks G W, Schlegel H B, Scuseria G E, Robb M A, Cheeseman J R, Scalmani G, Barone V, Mennucci B, Petersson G A, Nakatsuji H, Caricato M, Li X, Hratchian H P, Izmaylov A F, Bloino J, Zheng G, Sonnenberg J L, Hada M, Ehara M, Toyota K, Fukuda R, Hasegawa J, Ishida M, Nakajima T, Honda Y, Kitao O, Nakai H, Vreven T, Montgomery J A, Peralta J E, Ogliaro F, Bearpark M, Heyd J J, Brothers E, Kudin K N, Staroverov V N, Kobayashi R, Normand J, Raghavachari K, Rendell A, Burant J C, Iyengar S S, Tomasi J, Cossi M, Rega N, Millam M J, Klene M, Knox J E, Cross J B, Bakken V, Adamo C, Jaramillo J, Gomperts R, Stratmann R E, Yazyev O, Austin A J, Cammi R, Pomelli C, Ochterski J W, Martin R L, Morokuma K, Zakrzewski V G, Voth G A, Salvador P, Dannenberg J J, Dapprich S, Daniels A D, Farkas O, Foresman J B, Ortiz J V and Cioslowski J 2009 (Gaussian 09, revision D.01, Gaussian Inc.; Wallingford, CT USA)
41. Dennington R, Keith T and Millam J 2009 GaussView, Version 5. Semichem. Inc. Shawnee Mission, KS
42. Winterbourn C C 1995 Toxicity of iron and hydrogen peroxide: the Fenton reaction *Toxicol. Lett.* **82** 969
43. Munoz I G, Moran J F, Becana M and Montoya G 2005 The crystal structure of an eukaryotic iron superoxide dismutase suggests intersubunit cooperation during catalysis *Protein Sci.* **14** 387
44. Misra H P 1984 Inhibition of superoxide dismutase by nitroprusside and electron spin resonance observations on the formation of a superoxide-mediated nitroprusside nitroxyl free radical *J. Biol. Chem.* **259** 12678
45. Dumay A, Rincheval V, Trotot P, Mignotte B and Vayssière J L 2006 The superoxide dismutase inhibitor diethyldithiocarbamate has antagonistic effects on apoptosis by triggering both cytochrome c release and caspase inhibition *Free Rad. Biol. Med.* **40** 1377
46. Lengfelder E 1979 On the action of diethyldithiocarbamate as inhibitor of copper-zinc superoxide dismutase *Z. Naturforsch.* **34C** 1292
47. Sanz A M, Gómez-Contreras F, Navarro P, Sánchez-Moreno M, Boutaleb-Charki S, Campuzano J, Pardo M, Osuna A, Cano C, Yunta M J R and Campayo L 2008 Efficient inhibition of iron superoxide dismutase and of *trypanosoma cruzi* growth by benzo[*g*]phthalazine derivatives functionalized with one or two imidazole rings *J. Med. Chem.* **51** 1962

48. Sánchez-Moreno M, Gómez-Contreras F, Navarro P, Marín C, Ramírez-Macías, Rosales M J, Campayo L, Cano C, Sanz A M and Yunta M J 2015 *Parasitology* **142** 1115
49. Prasad A K and Mishra P C 2017 Catalytic action of Mn-superoxide dismutase in scavenging superoxide radical anion by double hydrogen abstraction from dihydrolipoic acid: A theoretical study *Int. J. Quant. Chem.* **117** e25355
50. Marcus R A 1964 Chemical and electrochemical electron transfer theory *Annu. Rev. Phys. Chem.* **15** 155
51. Marcus R A 1993 Electron transfer reactions in chemistry. Theory and experiment *Rev. Mod. Phys.* **65** 599
52. Marcus R A 1997 Electron transfer reactions in Chemistry. Theory and experiment *Pure App. Chem.* **69** 13
53. Nelsen S F, Blackstock S C and Kim Y 1987 Estimation of inner shell marcus terms for amino nitrogen compounds by molecular orbital calculations *J. Am. Chem. Soc.* **109** 677
54. Nelsen S F, Weaver M N, Luo Y, Pladziewicz J R, Ausman L K, Jentzsch T L and O'Konek J J 2006 Estimation of electronic coupling for intermolecular electron transfer from cross-reaction data *J. Phys. Chem. A* **110** 11665
55. Litwinienko G and Ingold K U 2003 Abnormal solvent effects on hydrogen atom abstractions. 1. The reactions of phenols with 2,2-Diphenyl-1-picrylhydrazyl (dpph) in alcohols *J. Org. Chem.* **68** 3433
56. Litwinienko G and Ingold K U 2004 Abnormal solvent effects on hydrogen atom abstraction. 2. Resolution of the curcumin antioxidant controversy. The role of sequential proton loss electron transfer *J. Org. Chem.* **69** 5888
57. Litwinienko G and Ingold K U 2005 Abnormal solvent effects on hydrogen atom abstraction. 3. Novel kinetics in sequential proton loss electron transfer chemistry *J. Org. Chem.* **70** 8982